

Characterization and Modeling of Metal/Double-Insulator/Metal Diodes for Millimeter Wave Wireless Receiver Applications

Stephen Rockwell¹, Derrick Lim¹, Bruce A. Bosco¹, Jeffrey H. Baker¹, Blake Eliasson², Keith Forsyth², Michael Cromar²

¹Motorola Labs, Tempe, AZ, 85284, Email: steve.rockwell@ieee.org

²Phiar Corp, Boulder, CO, 80301, eliasson@ieee.org

Abstract — In this paper we present measurements, models, and circuit implementations for a new low cost, thin film, metal/double-insulator/metal (MIIM) based tunneling diode technology. The device technology uses two insulators to form a tunneling device with very high speed performance capability, and is potentially compatible with many substrate technologies. This technology can potentially reduce cost, size, and improve performance for applications associated with high-speed communications, automotive collision avoidance and navigation, and homeland security weapons detection. Measured results of DC, S-parameter, and responsivity measurements in the 60 GHz band will be presented, including unmatched responsivity at 60 GHz of over 1000 V/W at -20dBm, which is competitive with detector diodes on GaAs or Sb-based materials. ADS-compatible non-linear models are developed and demonstrated, and an envelope detector design and results is presented.

Index Terms — Diodes, millimeter wave, MIM devices, thin film devices, sensitivity, responsivity, detector, 60GHz,

I. INTRODUCTION

Emerging markets targeting available unlicensed spectrum at millimeter wave frequencies require low cost solutions for widespread commercial deployment. Implementation of carefully engineered tunneling devices in thin film electronics has the potential to allow higher levels of integration on silicon ICs and potentially on lower cost materials as well.

In this paper, we report on the development a building block device in the form of a detector diode for high speed, high frequency thin film electronics which does not require crystalline semiconductor materials, and can be fabricated using standard IC planar lithographic techniques.

The objective of this work is to demonstrate the feasibility of these devices for applications requiring good responsivity to high frequency modulated carrier signals. Specifically, a demodulator for an amplitude shift key (ASK) receiver used in a millimeter wave high speed wireless link is identified as a practical application of this technology. This receiver is capable of multi-gigabit per second throughput. The characterization, modeling, simulation, and implementation of Phiar's MIIM devices targeting this receiver application are presented here.

II. DEVICE TECHNOLOGY

The millimeter wave wireless demodulator is based upon Phiar's metal/double-insulator/metal technology. Specifically, the MIIM diode provides the nonlinear rectifying element. MIIM diodes are based on quantum mechanical tunneling through thin (1-5nm) insulators. The device does not use semiconductors and is not limited by slower band conduction processes present in those materials. Rather, conduction by electron tunneling allows the intrinsic diode to operate at very high frequencies, in principle, well above 1 THz. The electrodes of the device itself (adjacent to the insulators) are metallic and can have very low parasitic resistance.

The device fabrication process is CMOS-compatible and because the materials are amorphous, may be realized upon on a variety of substrates (inter-layer dielectric material, thermally grown or deposited SiO₂, chemically mechanically polished SiO₂ on top of existing CMOS circuitry, fused quartz wafers, and polyimide for example). To date, performance of Phiar's MIIM devices has been limited by parasitics. The present devices were designed to operate at 60 GHz.

The uniqueness of the present diode structure over earlier MIM (single insulator) technologies is the use of two differing insulators adjacent to one-another [1]. The two insulators provide an increased nonlinearity in the current-voltage characteristic (lower differential resistance and higher responsivity). This performance advantage may be realized as a result of a quantum well that may be formed at the interface of the two insulators under forward bias.

III. CHARACTERIZATION

A. DC Characterization

DC current vs. voltage I(V) characteristics provide the first insight into device performance. The MIIM diode's DC current-density vs. voltage J(V) characteristics are shown in Fig. 1. For a junction size of 300 nm x 300 nm, the full scale current density of 2.5E+05 A/cm² corresponds to a current magnitude of 225μA and a zero bias differential resistance of 211 k .

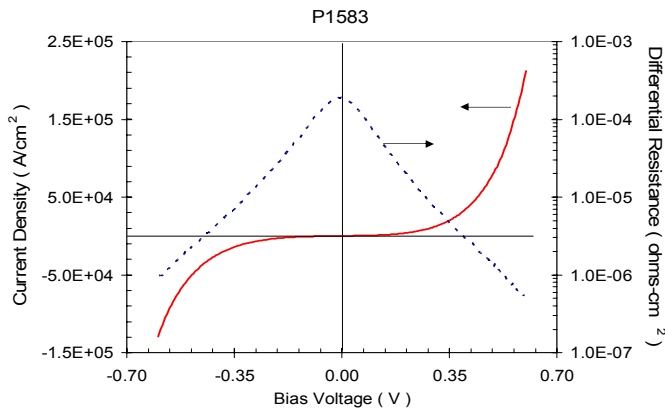


Fig. 1. The measured P1583 diode current density as a function of voltage (solid) and differential resistance (dashed).

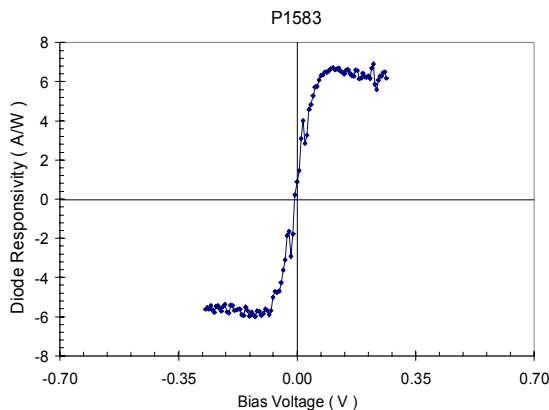


Fig. 2. The P1583 diode’s responsivity as a function of voltage as calculated from the DC I(V) curve.

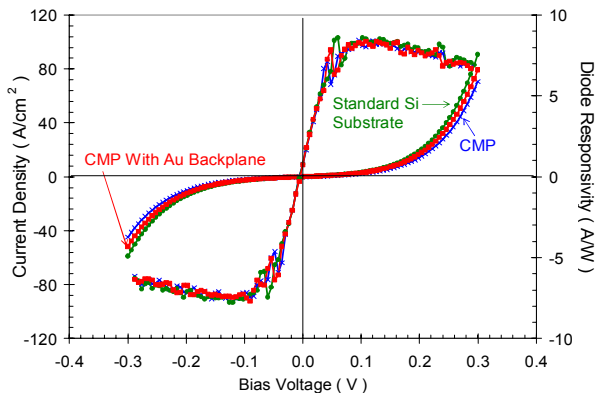


Fig. 3. A demonstration of a P1374 MIIM diode process repeated on three different substrates: a standard oxidized Si wafer (circle), a chemically mechanically polished deposited oxide (x), and a metallic backplane with chemically mechanically polished deposited oxide (square).

Current magnitudes are a function of the oxide thicknesses and physical materials properties. Through use of different device structures a variety of J(V) curves can be realized.

The diode responsivity, defined as one-half the second derivative of the DC current with respect to voltage multiplied

by the differential resistance, of the P1583 diode peaks at approximately 6.7 A/W under a forward bias of 0.1 V. The desired bias voltage for operation is selected by finding the voltage that provides the best combination of diode responsivity and differential resistance.

B. RF Characterization

Characterization devices were laid out for on wafer probing using a coplanar waveguide (CPW) feed network as shown in Fig. 4.. Device layout is optimized to minimize parasitics that could affect high frequency performance..

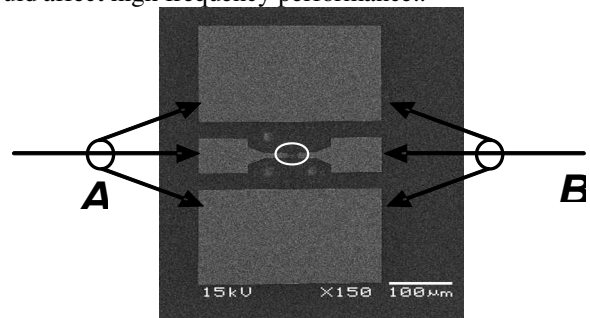


Fig. 4. An SEM micrograph of the CPW structure with diode (circled). Input A and output B probes are depicted.

The magnitude of the parasitics was extracted from s-parameter measurements on actual devices and calibration structures using an Anritsu 37397 vector network analyzer VNA.

The system responsivity of the diodes was independently tested in two labs. In both cases the setup was similar to the following. An Anritsu VNA was used as 60 GHz source. The RF path was composed of Port 1 from the VNA connected through an Anritsu V241C power splitter to an Anritsu V252 bias-t. The bias-t was connected through GSG probes to the MIIM diode input, point A. On the return side of the MIIM diode, point B, was connected to GSG probes, back through a second bias-t, power splitter, and returned to Port 2. The DC path, from the bias-t, is connected to a Keithley 2602 dual source meter acting as a bias voltage source for the MIIM diode preceding point A. The DC path of the bias-t following point B is connected to a load resistor with parallel capacitor and returned to the negative terminal of the 2602 source.

The response voltage is measured across the load resistor using the second channel on the Keithley 2602. The system responsivity is defined as the increase in voltage across the load resistor when the RF source is turned on. The RF power is measured using an Anritsu SC7278 calibrated power sensor connected to an Anritsu ML2438A power meter. The target incident power level is 10 μW (-20 dBm).

The measured system responsivity is a function of the MIIM junction size because of the RC time constant associated with the junction resistance and capacitance. System responsivity using a 1 G load resistor and three MIIM junction sizes is To a limit, smaller devices have higher responsivities due to a lower junction capacitance.

The load resistance in the test setup has an effect on the measured system responsivity as shown in the Fig. 6 for a single diode measured with five different load resistances.

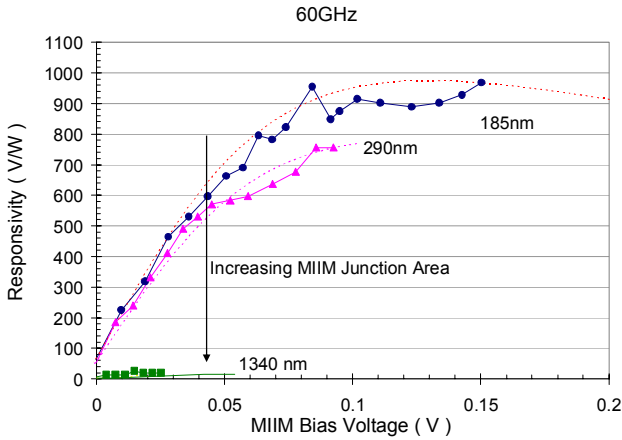


Fig. 5. Experimental system responsivity of three P1424 MIIM diodes of different sizes. The area dependence of the system responsivity is consistent with theory (dashed).

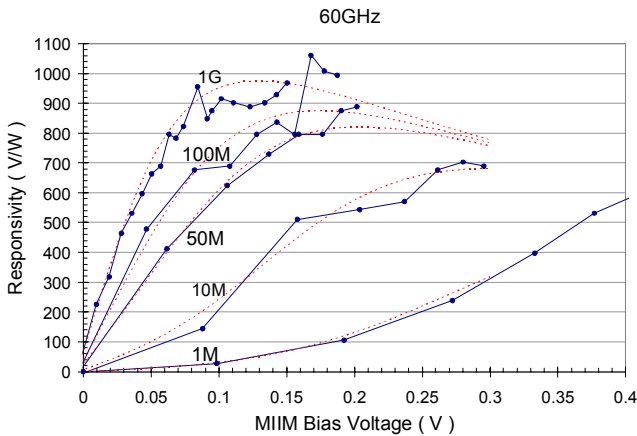


Fig. 6. Experimental system responsivity of a P1424 MIIM diode as a function of load resistance. The dependence on load resistance is consistent with theory (dashed).

In both of the above figures, a simple lumped element circuit model was developed which used the measured DC I(V) curve of the diode, diode responsivity calculated from the DC I(V), and s-parameters to extract the parasitic values to calculate the expected system responsivity.

The responsivity measurements were carried out on P1583 diodes for variations in input power from 7 to 16 μ W and a frequency sweep from 10 to 60 GHz with level system responsivity for a junction size of 225 nm.

C. Benchmark Comparisons

To assess these MIIM diodes objectively, the performance of existing state of the art technologies is used as a benchmark. For the defined application, GaAs Schottky and tunneling device technologies such as antimonide based heterostructure devices [2] have proven to perform very well.

A GaAs based detector diode made by Avago Semiconductor [3] and designed for operation beyond 100GHz was chosen as a benchmark device for this purpose. The primary metric chosen for comparisons is responsivity in V/W under defined operating conditions of frequency, power level, source match, load impedance, and bias.

Under these conditions the benchmark devices were found to achieve maximum responsivity on the order of 700 to 800 V/W. MIIM devices tested under the same conditions yielded responsivity on the order of 900 to 1000 V/W.

A summary of the typical responsivity of benchmark device versus the MIIM device, and a plot of multiple MIIM devices across multiple wafers is shown in Fig. 7.

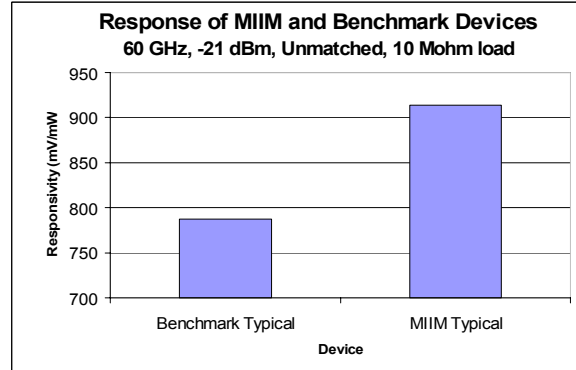


Fig. 7. Typical responsivity of the benchmark device vs. the MIIM devices.

IV. DEVICE MODELING

An equivalent circuit representation of the MIIM diode was developed in ADS, which facilitated the simulation of these devices in full circuits along with other elements of the design.

The voltage dependant current source component represents the DC I-V characteristics of the diode. It was found that the measured current as a function of the input voltage for the diode can be fitted to a power series expansion of the voltage. In ADS, this current-voltage relationship can be represented using a nonlinear resistor.

EM simulations and characterization of passive test structures yielded a parasitic capacitance of 5fF. The values of the remaining circuit elements were adjusted to measured S-parameter data. The small signal fit to the model is shown in Fig. 8.

The responsivity of the diode model also matches well to the measured data as shown in Fig. 9.

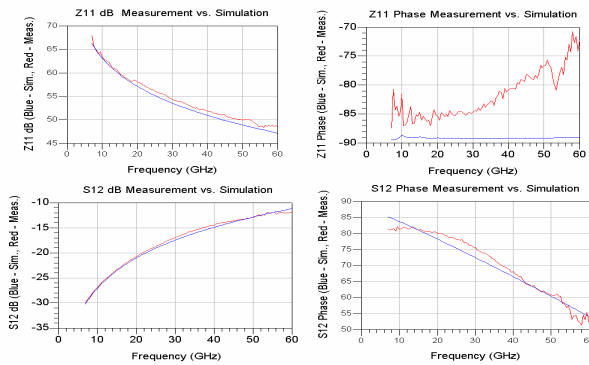


Fig. 8. Measured vs. modeled fit of Z and S parameters for MIIM diode.

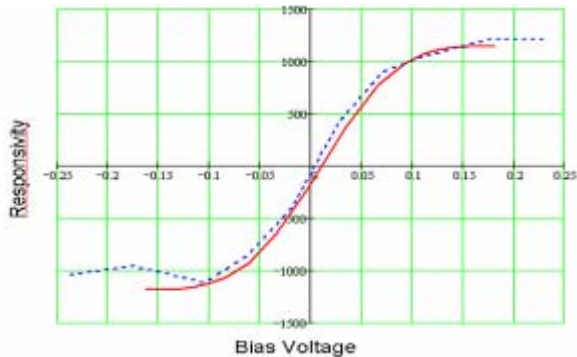


Fig. 9. Measured vs. modeled fit of diode responsivity at 60 GHz

V. DETECTOR DESIGN

A simple direct conversion receiver can be implemented with an antenna, a low noise amplifier and an envelope detector. The detector typically consists of a diode with good responsivity to the carrier frequency, a DC bias or current return path, input matching network, and output low pass or band pass filter.

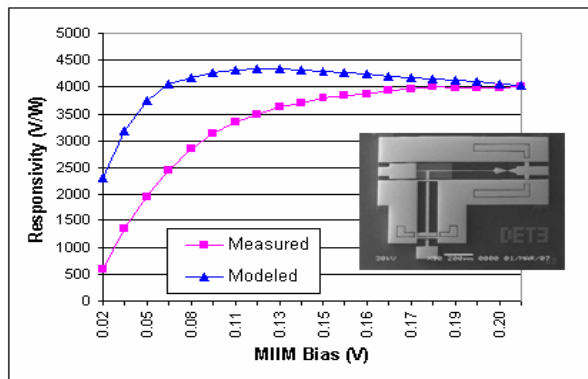


Fig. 10. Measured vs. modeled of integrated detector performance at 60 GHz -20 dBm input. Plotted vs. bias.

An integrated detector circuit was designed which includes input matching, a bias tee network, and an output band filter. The preliminary measured responsivity performance of these detectors at 60GHz with an input of -20 dBm was over 4000 V/W. The measured versus model and a photo of the circuit is shown in Fig. 10. Some discrepancy in lower bias fit to the model is under investigation

VI. FUTURE WORK

Other characteristics of this technology such as noise, temperature performance and reliability are being investigated. Additionally, one of the more promising aspects of this technology is process integration. Some work has already been performed to validate the feasibility of integration onto standard CMOS platforms. For this evaluation, completed devices were deposited with 1um of TEOS followed by planarization CMP. The planarized substrates were then processed through via lithography, etch and contact metallization. These results are shown in Fig. 3 Further development of integration into CMOS is expected.

VII. CONCLUSION

Next generation MIIM diodes are shown to exceed the performance of state of the art commercially available technology and may be integrated into millimeter wave receivers. The technology is compatible with multiple platforms and substrates and has the potential to greatly improve speed and simplify interconnects, both lowering cost and improving performance.

ACKNOWLEDGEMENT

The authors wish to acknowledge the characterization support by John Holmes of Motorola, and the efforts of the Phiar fabrication team: Jeff Bernacki, Derrick Carpenter, Olga Dmitriyeva, Rich Lew, Brandon Reese, and Jennifer Rossler for fabricating the devices used in these experiments. Additionally we would like to recognize the contributions of Steve Smith, Kurt Eisenbeiser, Tim Tighe, Yi Wei, and Rudy Emrick of Motorola.

REFERENCES

- [1] B. Eliasson, "Metal-Insulator-Metal Diodes for Solar Energy Conversion", *University of Colorado at Boulder*, 2001.
- [2] P. Fay, J. Schulman, S. Thomas, D. Chow, Y. Boegeman, K. Holabird, "High-Performance antimonide-based heterostructure backward diodes for millimeter-wave detection" *IEEE Electron Device Letters*, vol. 23, no. 10, October 2002.
- [3] Avago Semiconductor, 5988-6209EN, "HSCH-9161 Zero Bias Beam Lead Detector Diode".